

# Towards a Spiderman suit: large invisible cables and self-cleaning releasable superadhesive materials

**Nicola M Pugno**

Department of Structural Engineering, Politecnico di Torino, Corso Duca degli Abruzzi 24, 10129 Torino, Italy

E-mail: [nicola.pugno@polito.it](mailto:nicola.pugno@polito.it)

Received 9 February 2007, in final form 25 March 2007

Published 30 August 2007

Online at [stacks.iop.org/JPhysCM/19/395001](http://stacks.iop.org/JPhysCM/19/395001)

## Abstract

Spiders can produce cobwebs with high strength to density ratio and surprisingly display self-cleaning, strong and releasable adhesion (like geckos). Nanointerlocking, capillary and van der Waals forces, all potential adhesive mechanisms, are thus discussed, demonstrating the key role played by hierarchy in the design of superhydrophobic, i.e. self-cleaning (dry or wet and enhanced by activating Fakir drops as in lotus leaves) and superadhesive materials. The reversibility of the strong attachment is quantified thanks to an improved nonlinear peeling model including friction, for which the solution in closed form is provided. Thus, mimicking nature, thanks to carbon-nanotube-based technology, we suggest the feasibility of large invisible cables, as well as of self-cleaning, superadhesive and releasable hierarchical smart materials. We found that a man can theoretically be supported by a transparent cable with cross-section of 1 cm<sup>2</sup> and feasibly, with spider material gloves and boots, could remain attached even to a ceiling: a preliminary step towards a Spiderman suit.

(Some figures in this article are in colour only in the electronic version)

## 1. Introduction

The gecko's ability to 'run up and down a tree in any way, even with the head downwards' was first observed by Aristotle, almost 25 centuries ago, in his *Historia Animalium*. A comparable 'adhesive' system is found in spiders, that in addition have the ability of producing fascinating cobwebs.

In general, when two solid (rough) surfaces are brought into contact with each other, physical/chemical/mechanical attractions occur (see Bushan *et al* (1995)). The force developed that holds the two surfaces together is known as adhesion. Nanointerlocking (or friction), intermolecular forces, including capillary and van der Waals forces, suction, secretion of sticky fluids and electrostatic attraction are all potential adhesive mechanisms in biological attachment systems (see the review by Bhushan and Sayer (2007)).

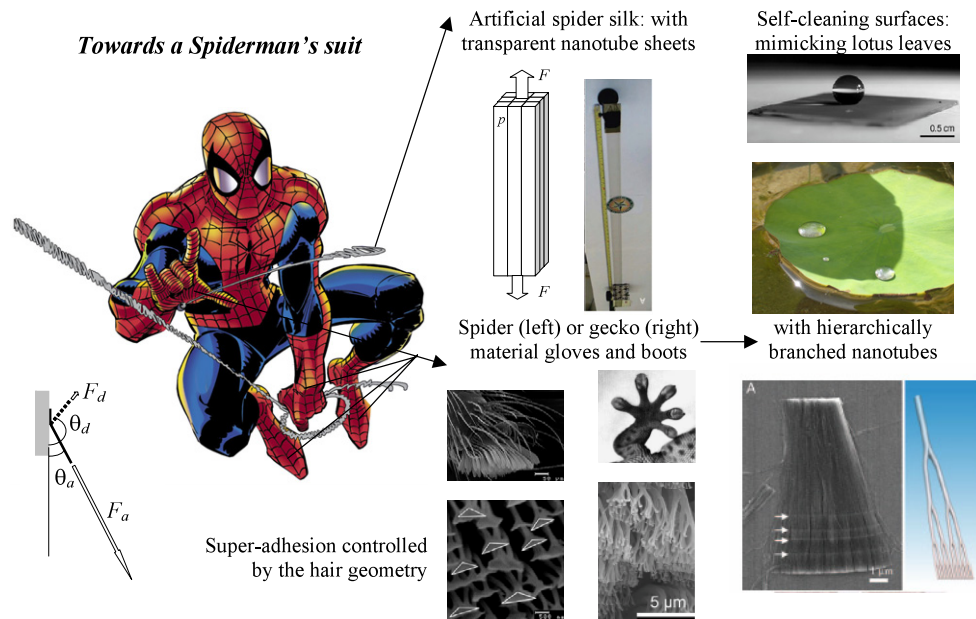


**Figure 1.** Spiderman (TM & © 2007 MARVEL.) must have large cobwebs and self-cleaning, superadhesive and releasable gloves and boots. Invisible large cables (Pugno 2006b) could be realized with nanotube bundles (related inset from (Zhang *et al* 2005)), whereas gloves and boots, mimicking spider (related inset from (Kesel *et al* 2004)) or gecko (related inset from (Gao *et al* 2005)) materials, with hierarchically branched nanotubes (related inset from (Meng *et al* 2005)) as suggested by our analysis. Note that the nanotube forest is superhydrophobic (water repellent) and thus self-cleaning (related inset from (Lau *et al* 2003)).

Suction cups operate under the principle of air evacuation; i.e., when they come into contact with a surface, air is forced out of the contact area, creating a pressure differential. The adhesive force generated is simply the pressure differential multiplied by the cup area. Thus, in our (sea level) atmosphere the achievable suction strength is  $\sigma_s \approx 0.1$  MPa, of the same order of magnitude as those observed in the aforementioned adhesive mechanisms or in spider/gecko adhesion. Even if suction can have an interesting role in producing synthetic adhesive materials, especially to be used in high-pressure environments, its mechanics is rather trivial. Moreover, although several insects and frogs rely on sticky fluids to adhere to surfaces, synthetic materials cannot evidently secrete these fluids without uncomfortable reservoirs. Furthermore, electrostatic attraction occurs only when two dissimilar heteropolar surfaces come into close contact. Accordingly, we will omit from our discussion these three mechanisms.

In geckos, the main adhesive mechanisms are capillary (Huber *et al* 2005a) and van der Waals (Autumn *et al* 2002) forces, whereas in spiders (Kesel *et al* 2004), in addition to the main van der Waals adhesion, nanointerlocking could have a role (e.g. during cobweb gripping). Accordingly, in this paper, we focus our attention on these three adhesive mechanisms, with an eye to the role played by hierarchy and to reversibility.

Hierarchical miniaturized hairs without adhesive secretions are characteristic features of both spiders and geckos. In jumping spider *Evarcha arcuata* (Kesel *et al* 2004), in addition to the tarsal claws (hooks with radius of  $\sim 50$   $\mu\text{m}$ ), a scopula (with surface area of 37 000  $\mu\text{m}^2$ ) is found at the tip of the foot; the scopula is differentiated in setae, each of them covered with numerous setules (with an average density of  $\sim 2.1$   $\mu\text{m}^{-2}$ ), terminating in a triangular contact (with surface area of  $\sim 0.17$   $\mu\text{m}^2$ ); see the related inset in figure 1. The total number of setules



**Figure 2.** Preliminary *in vivo* gecko experiments, performed on a gecko inside a Plexiglas box, suggest a safety factor of  $\sim 10$ , thus reduced by about one order of magnitude with respect to its ideal prediction, that is  $\sim 100$  (photographs by S Brianza).

per foot can be calculated at 78 000 and thus all eight feet are provided with a total of  $\sim 0.6$  million points of contact. The average adhesion force per setule was measured to be  $\sim 41$  nN, corresponding for the eight feet or scopulae to  $\sigma_{\text{spider}} \approx 0.24$  MPa and to a safety factor, that is the adhesive force over the body weight ( $\sim 15.1$  mg), of  $\lambda_{\text{spider}} \approx 173$  (Kesel *et al* 2004).

Similarly, a tokay gecko (*Gecko gecko*) foot consists of lamellae (soft ridges  $\sim 1$  mm in length), from which tiny curved setae ( $\sim 10$   $\mu\text{m}$  in diameter, density of  $\sim 0.014$   $\mu\text{m}^{-2}$ ) extend, each of them composed by numerous spatulae (100–1000 per seta,  $\sim 0.1$   $\mu\text{m}$  in diameter) with terminal contact units (having surface area of  $\sim 0.1$   $\mu\text{m}^2$ ) (Ruibla and Ernst 1965, Schleich and Kästle 1986). The adhesive force of a single seta and even of a single spatula has recently been measured to be respectively  $\sim 194$   $\mu\text{N}$  (Autumn *et al* 2000) or  $\sim 11$  nN (Huber *et al* 2005b). This corresponds to an adhesive strength of  $\sigma_{\text{gecko}} \approx 0.58$  MPa (Autumn *et al* 2000) and a safety factor of  $\lambda_{\text{gecko}} \approx 102$  (to compute this value we have assumed a weight of  $\sim 250$  g and a single foot surface area of  $\sim 110$   $\text{mm}^2$ ), comparable only with those of spiders ( $\sim 173$ , (Kesel *et al* 2004)), cocktail ants ( $> 100$ , (Federle *et al* 2000)) or knotgrass leaf beetles ( $\sim 50$ , (Stork 1983)).

Note that such safety factors are ideal and thus are expected to be reduced by about one order of magnitude (Pugno 2006a) as a consequence of the presence of ‘defects’, e.g. spurious particles, located at the contact interfacial zone. We have performed preliminary *in vivo* gecko experiments on a gecko inside a Plexiglas box (see figure 2), which have confirmed such a factor.

According to the previous values, we estimate for a gecko a total number of points of contacts of  $\sim 3$  billion, thus much larger than in spiders, as required by their larger mass (the number of contacts per unit area must scale as the mass to  $2/3$ ; see Arzt *et al* (2003)). The total adhesive force could easily be overcome by subsequently detaching single setules and not the whole foot at once (Niederegger and Gorb 2003).

Moreover, several natural materials exhibit superhydrophobicity, with contact angles between  $150^\circ$  and  $165^\circ$ ; often a strategy for allowing a safe interaction with water. This is the case for the leaves of about 200 plants, including asphodel, drosera, eucalyptus, euphorbia, *Ginkgo biloba*, iris, tulip and, perhaps the most famous, lotus (Neinhuis and Barthlott 1997, Barthlott and Neinhuis 1997). Similarly, animals can be superhydrophobic, as for the case of water strider legs, butterfly wings, duck feathers and bugs (Wagner *et al* 1996, Lee *et al* 2004, Gao and Jiang 2004). These surfaces are generally composed of intrinsic hydrophobic material and  $N = 2$  hierarchical micro-sized levels (Quéré 2005).

Superhydrophobia is extremely important in micro/nanofluidic devices for reducing the friction associated with the fluid flow, but also for self-cleaning: superhydrophobic materials

are often called self-cleaning materials since drops are efficiently removed taking with them the dirty particles which were deposited on them (Barthlott and Neinhuis 1997, Blossey 2003). This effect is extremely important in superadhesive materials. Hansen and Autumn (2005) have proved that gecko setae become cleaner with repeated (dry or wet) use; this is probably a consequence of the hierarchical nature of the gecko foot, as we are going to demonstrate.

A replication of the characteristics of gecko (Geim *et al* 2003) or spider feet would enable the development of a self-cleaning, like the lotus leaves (see the review by Quéré 2005), superadhesive and releasable hierarchical material and, with the conjunction of large invisible cables (Pugno 2006b), of a preliminary Spiderman suit (see figure 1, commented through the text).

## 2. Large invisible cables

In this section we present just an idea, no more, no less, for realizing large invisible cables (Pugno 2006b); a discussion on their technological feasibility is also included. The strength, stiffness and density of the invisible cable are estimated, and the condition of invisibility is provided.

Consider a rectangular cable having width  $W$ , thickness  $T$  and length  $L$ , the cross-section being composed of  $n \times m$  (multiwalled) carbon nanotubes with inner and outer diameter  $d_-$  and  $d_+$  respectively and length  $L$ . Let us assume that they are arranged in a square lattice with periodic spacing  $p = W/n = T/m$  (see figure 1, related inset). Then, the strength  $\sigma_C$  of the bundle, defined as the failure tensile force divided by the nominal area  $W \times T$ , is predicted as

$$\sigma_C = \frac{\pi}{4} \frac{d_+^2 - d_-^2}{p^2} \sigma_{NT}, \quad \sigma \rightarrow E, \rho \quad (1)$$

where  $\sigma_{NT}$  denotes the strength of the single carbon nanotube. To derive equation (1) we have assumed a full transfer load between the nanotube shells, which seems to be plausible if intertube bridgings are present, otherwise  $\sigma_{NT}$  would represent the nominal multiwalled nanotube strength. The same relationship is derived for the cable Young's modulus  $E_C$  considering in equation (1) the substitution  $\sigma \rightarrow E$  and  $E_{NT}$  as the Young's modulus of the single carbon nanotube. Similarly, the cable density  $\rho_C$ , defined as the cable weight divided by the nominal volume  $W \times T \times L$ , is predicted according to equation (1) with the substitution  $\sigma \rightarrow \rho$ , where  $\rho_{NT}$  would denote the carbon (nanotube) density. Thus, the same (failure) strain  $\varepsilon_C = \sigma_C/E_C = \sigma_{NT}/E_{NT}$  and strength over density ratio  $\sigma_C/\rho_C = \sigma_{NT}/\rho_{NT}$  is expected for the bundle and for the single nanotube. This ratio is huge, at least theoretically, e.g., as required in the megacable of the space elevator (Pugno 2006a). Thus, equation (1) is a law to connect the nanoscale properties of the single nanotube with the macroscopic properties of the bundle (with non-interacting nanotubes).

On the other hand, indicating with  $\lambda$  the light wavelength, the condition for a nanotube to be invisible is

$$d_+ \ll \lambda \quad (2a)$$

whereas to have a globally invisible cable we require in addition to not have interference between single nanotubes, i.e.

$$p \gg \lambda. \quad (2b)$$

We do not consider here the less strict limitations imposed by the sensitivity of the human eye, that can distinguish two different objects only if their angular distance is larger than  $\sim 1'$ . In other words, we want the cable to be intrinsically invisible.

Assuming  $d_+/\lambda \approx 1/10$ ,  $p/\lambda \approx 10$ , from the theoretical strength, Young's modulus and density of a single nanotube, we derive the following wavelength-independent invisible cable properties:

$$\sigma_C^{(\text{theo})} \approx 10 \text{ MPa}, \quad E_C \approx 0.1 \text{ GPa}, \quad \rho_C \approx 0.1 \text{ kg m}^{-3}. \quad (3)$$

Metre-long multiwalled carbon nanotube cables can already be realized (Zhang *et al* 2005), suggesting that our proposal could soon become technologically feasible. For such a nanostructured macroscopic cable, a strength over density ratio of  $\sigma_C/\rho_C \approx 120 - 144 \text{ kPa}/(\text{kg m}^{-3})$  was measured, dividing the breaking tensile force by the mass per unit length of the cable (the cross-section geometry was not of clear identification). Thus, we estimate for the single nanotube contained in such a cable  $\sigma_{\text{NT}} \approx 170 \text{ MPa}$  ( $\rho_{\text{NT}} \approx 1300 \text{ kg m}^{-3}$ ), much lower than its theoretical or measured nanoscale strength (Yu *et al* 2000). This result was expected as a consequence of the larger probability to find critical defects in larger volumes (see Carpinteri and Pugno 2005). Thus, defects limit the range of applicability of long bundles based on nanotubes, e.g. reducing their strength by about one order of magnitude (Pugno 2006a). However, the cable strength is expected to increase with the technological advancement. The cable density was estimated to be  $\rho_C \approx 1.5 \text{ kg m}^{-3}$  (Zhang *et al* 2005), thus resulting in a cable strength of  $\sigma_C \approx 200 \text{ kPa}$ . Note that a densified cable with a larger value of  $\sigma_C/\rho_C \approx 465 \text{ kPa}/(\text{kg m}^{-3})$  was also realized (Zhang *et al* 2005), suggesting the possibility of a considerable advancement for this technology in the near future. For such cables a degree of transparency was observed, confirming that our proposal is realistic. Inverting equation (1) we deduce for them  $p \approx 260 \text{ nm}$ , in good agreement with the scanning electron microscope (SEM) image analysis (Zhang *et al* 2005). The nanotube characteristic diameter was  $d_+ \approx 10 \text{ nm}$ . Considering the visible spectrum,  $\lambda \approx 400\text{--}600 \text{ nm}$ , condition (2a) was thus satisfied, whereas condition (2b) was not satisfied. Thus, only a partial degree of transparency was to be expected (see figure 1, related inset).

Moreover, multiwalled carbon nanotubes with  $d_+ \approx 50 \text{ nm}$  ( $d_- \approx 0 \text{ nm}$ ) spaced by  $p \approx 5 \mu\text{m}$  are expected to realize an invisible cable with the mechanical properties given in equation (3). For example, this would correspond to an invisible cable with a cross-section of  $1 \text{ cm}^2$  and weight per unit length of only  $10 \mu\text{g m}^{-1}$ , capable of supporting the weight of a man (1000 N). However, note that defects would decrease the cable strength, e.g., by one order of magnitude (Pugno 2006a).

The nanotubes will remain parallel, satisfying condition (2b), if the cable works under tension. A later force at the middle of the cable will tend to compact the nanotubes and at a strain of  $\varepsilon \approx 8(W/L)^2$  all of them will be in contact. Since for a cable  $W/L \ll 1$  (e.g.,  $10^{-2}$ ), a strain of the order of  $\varepsilon \approx 10^{-4}$ , i.e. small if compared with that at failure  $\varepsilon_{\text{NT}}^{(\text{theo})} \approx \sigma_{\text{NT}}^{(\text{theo})}/E_{\text{NT}} \approx 0.1$ , will activate the nanotube interaction. In such a situation the cable would 'appear' near to the point of application of the lateral force, i.e. where the condition of equation (2b) is not locally verified, to survive by activating the interaction; this behaviour could help in visualizing the cable after having trapped a victim.

Obviously, reducing the requirement of invisibility to that of (a degree of) transparency would automatically lead to stronger macroscopic synthetic cobwebs.

### 3. Nanohooks: the Velcro mechanics

In this section an estimation of the elastic strength of hooks (figure 3(a)) with friction is summarized (Pugno 2007), treating them as elastic arcs (see Carpinteri 1997). We have quantified, as the intuition and Velcro® material suggest, that hooks allow reversible strong attachment, establishing elastic-plastic or hyper-elastic behaviours as dictated by the

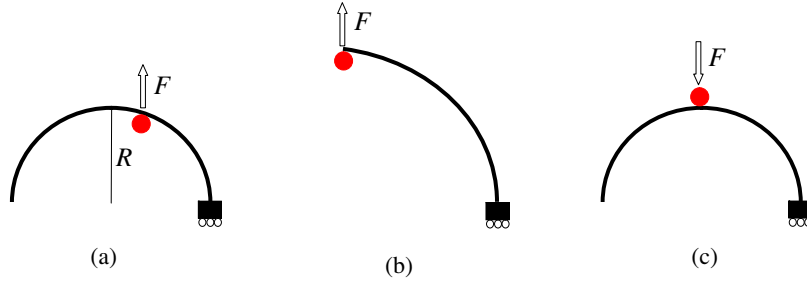


**Figure 3.** Elastic hook with friction. Conditions of interlocking (a), ultimate ‘elastic’ strength (b) and hauling (c).

competition between friction and large displacements (Pugno 2007). In addition, size effects suggest that nanocontacts are safer. Thus, we describe here the main results of a ‘Velcro nonlinear mechanics’ (Pugno 2007), that could also have interesting applications in different fields, as suggested by its recent observation in wood (Kretschmann 2003).

The hook elastic critical force  $F_h$  (figure 3(b)) can be estimated according to

$$F_h \approx \frac{(\pi/2 + \varphi)EI}{\pi R^2} \quad (4)$$

where  $\varphi$  is the friction coefficient between hook and substrate (or loop),  $E$  is the material Young modulus,  $I$  is the cross-sectional moment of inertia and  $R$  is the hook radius. Thus, if a number of hooks per unit area  $\rho_h = m/[\pi(2R)^2]$  is present, corresponding to an equivalent number  $m$  of hooks per clamp, the corresponding nominal strength will be

$$\sigma_h = \rho_h F_h = \frac{m(\pi/2 + \varphi)EI}{4\pi^2 R^4} = \frac{m(\pi/2 + \varphi)E}{16\pi(R/r)^4} \quad (5)$$

where  $r$  is the equivalent radius (in terms of inertia) of the cross-section. For example, considering  $m = 10$ ,  $\varphi = 0$ ,  $E = 10$  GPa (Young’s modulus for keratin material is  $E = 1 - 20$  GPa, see Russell (1986) and Bertram and Gosline (1987)) and  $R/r = 10$  corresponds to  $\sigma_h \approx 0.3$  MPa, comparable with the strength observed in *Evarcha arcuata* spiders of  $\sim 0.24$  MPa Kesel *et al* (2004); note the two spider hooks in the related inset of figure 1.

On the other hand, the maximum force for hooking (figure 3(c)) is

$$F_h^* = -\frac{\varphi EI}{R^2}. \quad (6)$$

Consequently the ratio

$$\mu = \frac{F_h}{|F_h^*|} = \frac{1}{\pi} + \frac{1}{2\varphi} \quad (7)$$

is expected to be very large ( $\mu(\varphi \rightarrow 0) \rightarrow \infty$ ), and thus strong and ‘reversible’ adhesion is expected in hooked materials. This can be easily verified by home-made experiments on Velcro materials, directly measuring  $\mu$  and thus deducing the related friction coefficient  $\varphi$ . For example, for  $\mu \approx 10 - 100$ ,  $\varphi \approx 5 \times 10^{-(2-3)}$ .

If a contact area  $A$  supports the (e.g. animal body) weight  $W$ , the safety factor, i.e. the ratio between the attachment force and the weight  $W = Mg = \rho Vg = \rho ALg$  ( $\rho$  is the density,  $g$  is the gravitational acceleration,  $V$  is the body volume and  $M$  its mass) is

$$\lambda = \frac{\sigma_h A}{W} = \frac{1}{\rho g} \frac{\sigma_h}{L} \quad (8)$$

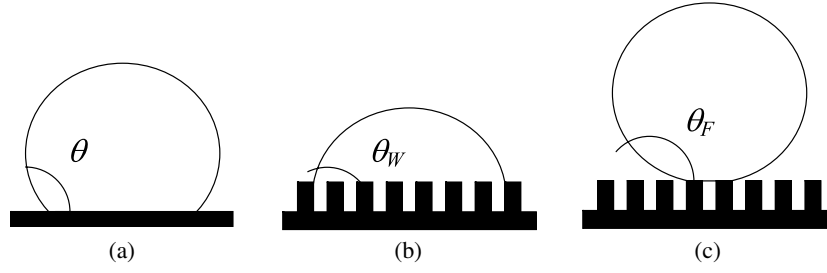


**Figure 4.** Contact angles for a drop on a flat surface (a) or on a rough surface in the Wenzel (b) or Fakir (c) state.

in which  $L = V/A$  is a characteristic size of the supported weight. Thus, smaller is safer. For example, since we expect  $L \propto M^{1/3}$ , roughly assuming  $\sigma_h \approx \text{const}$ , the predicted scaling is  $\lambda = kM^{-1/3}$ ; noting that in the *Evarcha arcuata* spiders (Kesel *et al* 2004)  $\lambda_{\text{spider}} \approx 173$  and  $M_{\text{spider}} \approx 15$  mg, we deduce  $k_{\text{spider}} \approx 43 \text{ g}^{1/3}$ . Thus for a Spiderman ( $M_{\text{man}} \approx 70$  kg), defined as a man having gloves and shoes composed of spider material, we roughly (because self-similarity is assumed) expect  $\lambda_{\text{Spiderman}} \approx 1$ . For gecko gloves, since for geckos  $\lambda_{\text{geckos}} \approx 102$  and  $M_{\text{geckos}} \approx 250$  g, we would deduce  $k_{\text{geckos}} \approx 643 \text{ g}^{1/3}$  and thus  $\lambda_{\text{Spiderman}} \approx 15$ . Accordingly, such gloves are sufficient to support Spiderman even on a ceiling.

The force carried by one hook scales as  $F_1 \equiv F_h \propto r^4/R^2$ , thus the bending, tensile and nominal stresses in the hook must scale as  $\sigma_b \propto r/R$ ,  $\sigma_t \propto (r/R)^2$  and  $\sigma_h \propto (r/R)^4$  respectively. Accordingly, size effects can be predicted. For example, splitting up the contact into  $n$  sub-contacts, i.e.  $R \rightarrow R/\sqrt{n}$ , would result in a force  $F_n = n^\beta F_1$  with  $\beta = 0$  if  $r \propto R$  but  $\beta = 2$  if  $r = \text{const}$ . Thus, for this last case, sub-contacts are found to be stronger, even if the hook will be more highly stressed and its mechanical strength will impose a lower bound to the radius of the smallest hook. This explains why nature uses nanosized bio-contacts, since usually  $0 < \beta < 2$ , as recently discussed on the basis of contact mechanics (for which  $\beta = 1/2$ , see Arzt *et al* (2003)). In the appendix it is shown that this enhancement cannot continue *ad infinitum* (Gao *et al* 2005). If the hook weight is a constant fraction of the body weight, the scaling of the safety factor is  $\lambda \propto r^2/R^3$ , similarly to the prediction of equation (8).

Finally, the work of adhesion  $\gamma_h$  per unit area can be computed according to

$$2\gamma_h = \rho_h \int_0^{F_h} \delta(F) dF = \left(\frac{1}{2} + \kappa\right) \sigma_h \delta(F_h) \quad (9)$$

where  $\delta$  is the force displacement and  $\kappa = 0$  for linear systems. For example, considering  $\kappa = 0$ ,  $\sigma_h = 0.3$  MPa as previously computed and  $\delta(F_h) \approx R = 100$  nm, we get  $\gamma_h \approx 0.03 \text{ N m}^{-1}$ , comparable with the work of adhesion observed in geckos ( $0.05 \text{ N m}^{-1}$ , see Autumn and Peattie (2002)).

#### 4. Superhydrophobic (/hydrophilic) and superattractive (/repulsive) surfaces: the hierarchical Wenzel's model

The contact angle (figure 4(a)) between a liquid drop and a solid surface was found by Young (1805) according to  $\cos \theta = (\gamma_{SV} - \gamma_{SL})/\gamma_C$ , where  $\gamma_C \equiv \gamma_{LV}$  and the subscripts of the surface tensions describe the solid (S), liquid (L) and vapour (V) phases. Note that for  $(\gamma_{SV} - \gamma_{SL})/\gamma_C > 1$  the drop tends to spread completely on the surface and  $\theta = 0^\circ$ , whereas for  $(\gamma_{SL} - \gamma_{SV})/\gamma_C > 1$  the drop is in a pure non-wetting state and  $\theta = 180^\circ$ . According to the well known Wenzel's model (1936, 1949), the apparent contact angle  $\theta_W$

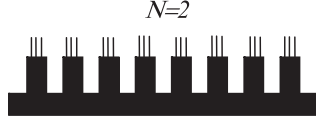


**Figure 5.** A hierarchical surface with  $N = 2$  levels.

is a function of the surface roughness  $w$ , defined as the ratio of rough to planar surface areas, namely,  $\cos \theta_W = w \cos \theta$  (figure 4(b)). The apparent contact angle also varies with the heterogeneous composition of the solid surface, as shown by Cassie and Baxter (1944). Consider a heterogeneous surface made up of different materials characterized by their intrinsic contact angles  $\theta_i$  and let  $\varphi_i$  be the area fraction of each of the species; the individual areas are assumed to be much smaller than the drop size. Accordingly, the apparent contact angle  $\theta_{CB}$  can be derived as  $\cos \theta_{CB} = \sum_i \varphi_i \cos \theta_i$  (Cassie and Baxter 1944).

A droplet can sit on a solid surface in two distinct configurations or states (figures 4(b) and (c)). It is said to be in the Wenzel state (figure 4(b)) when it is conformal with the topography. The other state in which a droplet can rest on the surface is called the Fakir state, after Quéré (2002), where it is not conformal with the topography and only touches the tops of the protrusions on the surface (figure 4(c)). The observed state should be the one of smaller contact angle, as can be evinced by energy minimization (Bico *et al* 2002).

Let us consider a hierarchical surface (figure 5). The first level is composed by pillars in fraction  $\varphi$  (as in figures 4(b) and (c)). Each pillar is itself structured in  $n$  sub-pillars in a self-similar (fractal) manner, and so on. Thus, the pillar fraction at the hierarchical level  $N$  is  $\varphi^N$ , whereas the related number of pillars at the level  $N$  is  $n^N$ . Applying the Cassie and Baxter law (Cassie and Baxter 1944) for the described composite (solid/air) hierarchical surface (the contact angle in air is by definition equal to  $180^\circ$ ), we find for the hierarchical Fakir state

$$\cos \theta_F^{(N)} = \varphi^N (\cos \theta + 1) - 1. \quad (10)$$

Note that for  $\cos \theta_F^{(0)} = \cos \theta$  as it must be, whereas for  $\cos \theta_F^{(1)} = \varphi (\cos \theta + 1) - 1$ , as already deduced for the case described in figure 4(c) (Bico *et al* 1999). Equation (10) quantifies the crucial role of hierarchy and suggests that hierarchical surfaces are fundamental to realize superhydrophobic materials (effective contact angle larger than  $\theta_{SHpho} \approx 150^\circ$ ), since we predict  $\theta_F^{(\infty)} = 180^\circ$ . The minimum number of hierarchical levels necessary to achieve superhydrophobia in the Fakir state is thus

$$N_{SHpho}^{(F)} = \frac{\log \left( \frac{1 + \cos \theta_{SHpho}}{1 + \cos \theta} \right)}{\log \varphi} \quad (11)$$

and the logarithmic dependence suggests that just a few hierarchical levels are practically required.

By geometrical argument the roughness  $w$  of the introduced hierarchical surface (figure 5) can be calculated in closed form. The roughness at the hierarchical level  $k$  is given by  $w^{(k)} = 1 + S_L^{(k)}/A$ , in which  $A$  is the nominal contact area and  $S_L^{(k)}$  is the total lateral surface area of the pillars. The pillar at the level  $k$  has an equivalent radius  $r_k$  and a length  $l_k$  and the pillar slenderness  $s$ , defined as the ratio between its lateral and base areas, is  $s = 2l_k/r_k$ . The air surface area at the level  $k$  can be computed as  $A(1 - \varphi^k)$  or equivalently as  $A - n^k \pi r_k^2$ , thus we deduce  $r_k = r_0(\varphi/n)^{k/2}$ , with  $A \equiv A_0 \equiv \pi r_0^2$ . Consequently,

$$w^{(N)} = 1 + \frac{1}{\pi r_0^2} \sum_{k=1}^N 2\pi r_k l_k n^k = 1 + s \sum_{k=1}^N \varphi^k = 1 + s \frac{\varphi - \varphi^{N+1}}{1 - \varphi} \forall n. \quad (12)$$

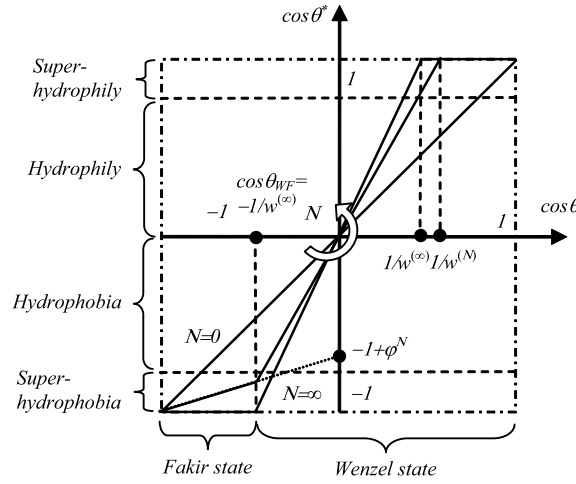


**Figure 6.** Effective contact angle  $\theta^* = \theta_{F,W}^{(N)}$  as a function of the intrinsic one  $\theta$  by varying the number  $N$  of hierarchical levels. Thus, superhydrophobic/hydrophilic surfaces can be obtained by an opportune design of the hierarchical architecture, according to this phase diagram or reported equations (note that metastable Fakir drops could also be observed in the Wenzel region (dotted line); see Quéré (2005)).

Note that the result becomes independent from  $n$  (and that  $w^{(0)}(\varphi) = 1 = w^{(N)}(\varphi = 0)$ ,  $w^{(1)} = 1 + s\varphi$ , whereas  $w^{(N \neq 1)}(\varphi = 1) = \infty$ ). Thus we find for the hierarchical Wenzel state

$$\cos \theta_W^{(N)} = w^{(N)} \cos \theta = \left( 1 + s \frac{\varphi - \varphi^{N+1}}{1 - \varphi} \right) \cos \theta. \quad (13)$$

Equation (13) suggests that hierarchical surfaces can also be interesting to realize superhydrophilic materials, since we predict  $\cos \theta_W^{(\infty)} = w^{(\infty)} \cos \theta$  with  $w^{(\infty)} = 1 + s\varphi/(1 - \varphi)$ ; thus if  $\cos \theta > 0$ ,  $\theta_W^{(\infty)} \rightarrow 0$ , for  $s \rightarrow \infty$  or  $\varphi \rightarrow 1$ . However, note that for  $\cos \theta < 0$ ,  $\theta_W^{(\infty)} \rightarrow 180^\circ$  ( $s \rightarrow \infty$  or  $\varphi \rightarrow 1$ ), and thus superhydrophobia can also occur in the Wenzel state, without invoking Fakir drops. The minimum number of hierarchical levels necessary to render the surface superhydrophobic/hydrophilic in the Wenzel state is thus

$$N_{SHpho,phi}^{(W)} = \frac{\log \left( 1 + \frac{(1-\varphi)}{s\varphi} \left( 1 - \frac{\cos \theta_{SHpho,phi}}{\cos \theta} \right) \right)}{\log \varphi} \quad (14)$$

where effective contact angles smaller than  $\theta_{SHpho,phi}$  define superhydrophilicity.

Comparing  $\theta_W^{(N)}$  and  $\theta_F^{(N)}$ , we find that the Fakir state is activated at each hierarchical level for (we omit here second order problems, related to metastability, contact angle hysteresis and the limit of Wenzel's approach, for which the reader should refer to the review by Quéré (2005))

$$\theta > \theta_{WF}, \quad \cos \theta_{WF} = -\frac{1 - \varphi^N}{w^{(N)} - \varphi^N} = -\frac{1}{w^{(\infty)}} = -\frac{1 - \varphi}{1 + \varphi(s - 1)} \forall N. \quad (15)$$

Note that the result is independent of  $N$  and  $\theta_{WF} \rightarrow 90^\circ$  for  $s \rightarrow \infty$  or  $\varphi \rightarrow 1$ , and thus a hydrophobic/hydrophilic material composed by sufficiently slender or spaced pillars surely will (will not) activate Fakir drops and will become superhydrophobic(hydrophilic) for a large enough number of hierarchical levels. Thus hierarchy can enhance an intrinsic property of a material. The role of hierarchy is summarized in the phase diagram of figure 6.

For example, for plausible values of  $\varphi = 0.5$  and  $s = 10$  we find from equation (15)  $\theta_{WF} = 95.2^\circ$ ; thus, assuming  $\theta = 95^\circ$ , the Fakir state is not activated and the Wenzel state prevails (if the Fakir state still prevails it is metastable; see Quéré (2005)). From equation (12)  $w^{(1)} = 6$ ,  $w^{(2)} = 8.5$ ,  $w^{(3)} = 9.75$  and  $w^{(4)} = 10.375$ ; accordingly, from equation (13)  $\theta_W^{(1)} \approx 122^\circ$ ,  $\theta_W^{(2)} \approx 138^\circ$ ,  $\theta_W^{(3)} \approx 148^\circ$  and  $\theta_W^{(4)} \approx 155^\circ$ , thus  $N = 4$  hierarchical levels are required for activating superhydrophobia (from equation (14)  $N_{\text{SHpho}}^{(W)} = 3.2$ ). On the other hand, assuming  $\theta = 100^\circ$ , Fakir drops are activated and from equation (10)  $\theta_F^{(1)} \approx 126^\circ$ ,  $\theta_F^{(2)} \approx 143^\circ$  and  $\theta_F^{(3)} \approx 154^\circ$ , thus  $N = 3$  hierarchical levels are sufficient to achieve superhydrophobia (from equation (11)  $N_{\text{SHpho}}^{(F)} = 2.6$ ).

Some insects, such as the beetle *Hemisphaerota cyanea*, use capillary to stick to their substrate, generating a force close to 1 g (i.e. 60 times its body mass) for more than 2 min (Eisner and Aneshansley 2000), allowing them to resist attacking ants; tokay geckos use the same principle (in addition to van der Waals forces) to generate their tremendous adhesion (Huber *et al* 2005a).

Between a spherical surface (contact angle  $\theta$ ) of radius  $r_0$  and a flat plate (contact angle  $\theta_p$ ), the capillary attractive or repulsive force is predicted to be  $F_C = 2\pi r_0 \gamma_C (\cos \theta + \cos \theta_p)$  (McFarlane and Tabor 1950). Thus, for a pillar of size  $r_0$  composed of  $N$  hierarchical levels, the force is  $F_C^{(N)} = n^N 2\pi r_N \gamma_C (\cos \theta + \cos \theta_p)$  and the nominal strength  $\sigma_C^{(N)} = F_C^{(N)} / (\pi r_0^2)$  becomes

$$\sigma_C^{(N)} = \frac{2(\varphi n)^{N/2}}{r_0} \gamma_C (\cos \theta_{W,F}^{(N)} + \cos \theta_p). \quad (16)$$

Note that for  $N = 0$  such a capillary strength corresponds to the classical capillary strength. For  $N = 1$  the strength scales as  $\sqrt{n}$ , in agreement with a recent discussion (Arzt *et al* 2003): splitting up the contact into  $n$  sub-contacts would result in a stronger interaction (with a cut-off at the theoretical strength); smaller is stronger (see Carpinteri and Pugno 2005). This explains the observed miniaturized size of biological contacts. Introducing the previously computed contact angle related to the hierarchical surface allows one to evaluate the hierarchical capillary force, with or without activation of the Fakir state. Superattraction/repulsion can thus be achieved thanks to hierarchy, since  $\sigma_C^{(N)} \approx \sigma_C^{(0)} (\varphi n)^{N/2}$ .

Thus, the analysis demonstrates and quantifies that superhydrophobic/hydrophilic and simultaneously superattractive/repulsive surfaces can be realized, mimicking nature thanks to hierarchical architectures. Assuming  $\varphi = 0.5$ ,  $n = s = 10$  and  $\theta \approx 120^\circ$  (as in lotus leaves), the analysis shows that Fakir drops are activated and only two hierarchical levels are required to achieve superhydrophobia ( $\theta > \theta_{WF} = 95.2^\circ$ ,  $N_{\text{SHpho}}^{(F)} = 1.9$ ;  $\theta_F^{(1)} \approx 139^\circ$ ,  $\theta_F^{(2)} \approx 151^\circ$ ), in agreement with direct observations on superhydrophobic plants (see the discussion in section 1). Simultaneously, we deduce  $\sigma_C^{(1)} \approx 2.2\sigma_C^{(0)}$ ,  $\sigma_C^{(2)} \approx 5.0\sigma_C^{(0)}$  and  $\sigma_C^{(3)} \approx 11.2\sigma_C^{(0)}$ , i.e. just three hierarchical levels (or even two, if  $\varphi \approx 1$  and  $n \approx 10$ ) are sufficient to enhance the capillary strength by one order of magnitude, generating superattractive ( $\sigma_C^{(0)} > 0$ ) or super-repulsive ( $\sigma_C^{(0)} < 0$ ) surfaces. Thus, the analysis suggests the feasibility of innovative self-cleaning and simultaneously superadhesive hierarchical tissues, as observed in spiders and geckos.

Analogously, hierarchy simultaneously enhances the work of adhesion, and thus the corresponding force, per unit nominal area, due to the larger effective surface area. Accordingly, the maximum (assuming all the surfaces in contact) effective work of adhesion can be derived by the following energy equivalence:

$$\gamma_{\text{max}}^{(N_1, N_2)} \approx \gamma_C (w_1^{(N_1)} + w_2^{(N_2)}) \quad (17)$$

in which the subscripts 1 and 2 refer to the two surfaces in contact. For example, the adhesive

force between two-hierarchical level surfaces, defined by  $w_{1,2}^{(2)} = 1.75$  ( $\varphi = 0.5, s = 1$ ), is enhanced by hierarchy by a factor of 3.5 (with respect to the two corresponding flat surfaces). Note that for  $s = 10$  this factor becomes 18 and remains significantly larger than one (i.e. 10) even if one of the two surfaces becomes perfectly flat.

## 5. Capillary and van der Waals forces

The capillary force can also be derived according to the well known Laplace's law (1847). The attractive force between two flat plates of area  $A$ , separated by a liquid of thickness  $t$ , with (liquid/vapour) surface tension  $\gamma_C$  and (liquid/solid) contact angle  $\theta$  is (see the review by Quéré 2005)

$$F_C = \frac{2A\gamma_C \cos \theta}{t}. \quad (18)$$

Note that  $\sigma_C = F_C/A$  is a function of the liquid thickness but not of the size of the contact. Considering for example  $\gamma_C = 0.05 \text{ N m}^{-1}$ ,  $\theta = 80^\circ$  and  $t = 1 \text{ nm}$  would yield  $\sigma_C \approx 9 \text{ MPa}$ . The force described by equation (17) is attractive for  $\theta < 90^\circ$  (hydrophilic) or repulsive for  $\theta > 90^\circ$  (hydrophobic). An additional viscous force can be generated  $F_C^{(\eta)} \propto \eta/\tau$ , where  $\eta$  is the dynamic viscosity of the liquid and  $\tau$  is the separation time interval.

Note the differences between the force predictions of equation (18) and that considered in the previous section (McFarlane and Tabor 1950), i.e.

$$F_C = 2\pi r_0 \gamma_C (\cos \theta + \cos \theta_P) \quad (19)$$

in the limit of  $r_0 \rightarrow \infty$ , which suggest that we are far from a full understanding of the mechanism. In addition, both the approaches predict  $\sigma_C = F_C/A = F_C/(\pi r_0^2) \rightarrow \infty$  for  $t, r_0 \rightarrow 0$  in contrast to the common sense of a finite theoretical strength  $\sigma_C^{(\text{th})}$ . This cut-off could be a consequence of a quantized (instead of a continuous) crack propagation, as discussed in the example reported in the appendix. Thus, the following asymptotic matching can be straightforwardly proposed:

$$\sigma_C \approx \left( \frac{2}{r_0 + c} + \frac{1}{t + c} \right) \gamma_C (\cos \theta + \cos \theta_P), \quad c \approx 3\gamma_C (\cos \theta + \cos \theta_P) / \sigma_C^{(\text{th})}. \quad (20)$$

Similarly, the van der Waals force between two parallel surfaces of area  $A$  is (Hamaker (1937); see also Israelachvili 1991)

$$F_{\text{vdW}} = \frac{HA}{6\pi t^3} \quad (21)$$

where  $H$  is the Hamaker's constant, with a typical value around  $10^{-20} \text{ J}$  (as before,  $t < 30 \text{ nm}$  is the separation between the two surfaces). Note that  $\sigma_{\text{vdW}} = F_{\text{vdW}}/A$  is a function of the liquid thickness but not of the size of the contact. Considering for example  $t = 1 \text{ nm}$  would yield  $\sigma_{\text{vdW}} \approx 0.5 \text{ MPa}$ .

For the case of a spherical surface of radius  $r_0$  and a flat plate, the contact force predicted according to the 'JKR' model of contact mechanics (Johnson *et al* 1971) is

$$F_{\text{vdW}} = 3/2\pi \gamma_{\text{vdW}} r_0. \quad (22)$$

Thus also in this case, as formerly discussed by Arzt *et al* (2003),  $F_n = \sqrt{n} F_1$ . Moreover, since  $F_{\text{vdW}} \propto r_0$  the results reported in the previous section are still applicable.

As for capillary action, the differences between the two approaches, summarized in equations (21) and (22), are evident, which suggests that we are again far from a full understanding of the mechanism. In addition, equations (21) and (22) predict

$\sigma_{vdW} = F_{vdW}/A = F_{vdW}/(\pi r_0^2) \rightarrow \infty$  for  $t, r_0 \rightarrow 0$  in contrast to the common sense of a finite theoretical strength  $\sigma_{vdW}^{(th)}$  (and of a quantized crack propagation, see the appendix). Again, an asymptotic matching can be proposed:

$$\sigma_{vdW} \approx 3/2\gamma_{vdW} \left( \frac{1}{r_0 + c} + \frac{H}{9\gamma_{vdW}\pi(t + c)^3} \right), \quad (23)$$

$$c = X(6\pi\sigma_{vdW}^{(th)}; -9\pi\gamma_{vdW}; 0; -H)$$

where  $X(a; b; c; d)$  denotes the solution of the third-order polynomial equation  $ax^3 + bx^2 + cx + d = 0$ , derived imposing  $c:\sigma_{vdW}(r_0, t \rightarrow 0) = \sigma_{vdW}^{(th)}$  (one could also consider valid equation (23) with  $c \rightarrow 0$ , with a cut-off at  $\sigma_{vdW}^{(th)}$ ). To have an idea of the theoretical strength note that  $\sigma_{vdW}^{(th)} \approx 20$  MPa (see Gao *et al* (2005)).

The different force predictions for plausible values are of the same order of magnitude. Using equation (22), as done by Autumn *et al* (2000), Arzt *et al* (2003) ( $\gamma_{vdW} \approx 0.05$  N m<sup>-1</sup>) for the gecko spatula ( $r_0 \approx 0.05$   $\mu$ m) we get  $F_{spatula} \approx 12$  nN, comparable to the observed value of  $\sim 11$  nN (Huber *et al* 2005b). Thus, for a seta composed by 1000 spatulae,  $F_{seta} \approx 12$   $\mu$ N ((Autumn *et al* 2000, 2002) measured values of  $\sim 194$   $\mu$ N and  $\sim 40$   $\mu$ N respectively); for a non-hierarchical seta from equation (22) one would deduce ( $r_0 \approx 5$   $\mu$ m)  $F_{seta}^I \approx 1.2$   $\mu$ N and thus for a real, thus hierarchical, seta having 1000 spatulae  $F_{seta} \approx \sqrt{1000} \times 1.2$   $\mu$ N  $\approx 38$   $\mu$ N. Similarly for the setule of a spider  $R_{eq} \approx \sqrt{0.17/\pi}$   $\mu$ m  $\approx 0.2$   $\mu$ m (terminal surface area of  $\sim 0.17$   $\mu$ m<sup>2</sup>) and  $F_{setule} \approx 47$  nN (observed value  $\sim 41$  nN, (Kesel *et al* 2004)).

Finally, we note that since different mechanisms could be simultaneously activated the real adhesive force (or strength or work) could be computed as

$$F = \sum_i F_i f_i \quad (24)$$

in which  $F_i$  is the force activated by the  $i$ th mechanism having weight  $f_i$  ( $\sum_i f_i = 1$ ).

For example, for geckos a still partially unsolved question is to quantify the participation of capillary and van der Waals forces in their adhesion (nanohook and suction mechanisms in geckos have been ruled out; see the review by (Bhushan and Sayer 2007)). We note that Huber *et al* (2005a) observed a humidity ( $U$ ) dependence of the adhesion force in gecko spatulae, thus, from equation (24) we could write

$$F = F_{dry} f_{dry} + F_{wet} f_{wet} \approx F_{vdW}(1 - U) + (F_{vdW} + F_C)U. \quad (25)$$

By fitting their data we find  $F_{vdW} \approx 7$  nN and  $F_C \approx 5$  nN, thus  $F_{vdW}/F_C \approx 1.4$ , i.e., van der Waals are expected to be the main adhesive forces in geckos even if capillary ones play a significant role too.

Equations (20) and (23) can be straightforwardly extended to hierarchical surfaces according to our findings reported in the section 4.

## 6. Releasable strong nonlinear adhesion

Consider the detachment as the peeling of a thin film of (free) length  $l$ , width  $b$  and thickness  $h$ , pulled at an angle  $\vartheta$  by a force  $F$  (figure 7). A non-linear stress-strain relationship  $\sigma = E(\varepsilon)\varepsilon$  is considered. The total potential energy (elastic energy minus external work) of the film is  $\Phi = bhl \int_0^\varepsilon E(\varepsilon)\varepsilon d\varepsilon - Fl(1 - \cos \vartheta + \varepsilon)$ . Thus, the energy release rate is

$$2\Delta\gamma \equiv -\frac{1}{b} \frac{d\Phi}{dl} = -h \int_0^\varepsilon E(\varepsilon)\varepsilon d\varepsilon + \frac{F}{b}(1 - \cos \vartheta + \varepsilon). \quad (26)$$

The detachment will take place when  $\Delta\gamma \equiv \gamma \equiv \gamma_1 + \gamma_2 - \gamma_{12}$ , where  $\gamma_{1,2}$  are the surface energies of the two materials in contact and  $\gamma_{12}$  is that of the interface.

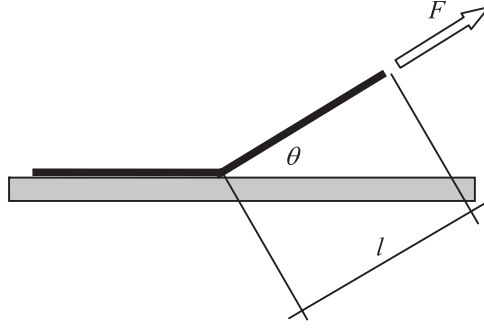


Figure 7. Peeling of a thin film.

For quadratic nonlinearities, i.e.  $E(\varepsilon) = E + E'\varepsilon$ , a closed form solution is still reachable. Note that  $E' < 0$  describes elastic–plastic materials (e.g. a hooked surface with  $\varphi > \varphi_C \approx \pi/39$ , see Pugno (2007)), whereas  $E' > 0$  hyper-elastic ones (e.g. a hooked surface with  $\varphi < \varphi_C$ ). The detachment force is found in the following form:

$$\varepsilon_C = X(4E'; 3E + 6E'(1 - \cos \vartheta); 6E(1 - \cos \vartheta); -12\gamma h), \quad F_C = AE(\varepsilon_C)\varepsilon_C \quad (27)$$

(as before  $X(a; b; c; d)$  denotes the solution of the third-order polynomial equation  $ax^3 + bx^2 + cx + d = 0$ ). For  $E' \rightarrow 0$  the classical Kendall (1975) prediction is recovered. Varying the pulling angle, strong force variations are found, as can easily be evinced considering the simplest case in the limit of  $E^{-1}$ ,  $E' \rightarrow 0$ , deducing  $F_C = 2\gamma b/(1 - \cos \vartheta)$ . Note that, also according to fracture mechanics, sub-contacts are safer ( $b \rightarrow b/\sqrt{n}$ ,  $F_n = \sqrt{n}F_1$ ; the appendix shows that this cannot be *ad infinitum*).

Moreover, the strongest attachment is achieved for  $\vartheta = 0$ , whereas the easiest detachment for  $\vartheta = \pi$ . The ratio between the corresponding forces is

$$\frac{F_a}{F_d} \equiv \frac{F_C(\vartheta = 0)}{F_C(\vartheta = \pi)} = g(E') \frac{1 + \sqrt{\chi + 1}}{\sqrt{\chi}}, \quad \chi \equiv \gamma/(hE) \quad (28)$$

where  $g(E')$  is a known function describing the constitutive nonlinearity, which could have an important role for soft matter, and in particular  $g(0) = 1$ ; in this case  $F_a/F_d \rightarrow 1, \infty$  for  $\chi \rightarrow \infty, 0$ . For example, taking  $\gamma = 0.05 \text{ N m}^{-1}$  (of the order of the previously discussed  $\gamma_{h,c,vdW}$ ),  $h = 100 \text{ nm}$ ,  $E = 10 \text{ GPa}$  we find  $F_a/F_d \approx 283$ . *This value is of the same order of magnitude as the safety factor found in spiders* (Kesel *et al* 2004), *i.e.* 173. Such a geometrical control can thus explain the smart safety factor reduction during detachment up to  $\sim 1$ , needed for the animal to walk. Thus, this pulling angle control can represent the main mechanism to achieve reversible adhesion. For example, for a man with adhesive gloves capable of supporting 300 kg at  $\vartheta \approx \pi$ , only  $\sim 1 \text{ kg}$  must be applied at  $\vartheta \approx 0$  to detach them (an articulated system to enhance the wrist (and ankle) rotation could thus be required). Probably the proper use of such hypothetical gloves and boots would require appropriate training, similarly to the use of a pair of skis, a paraglider or a wet suit.

The value of  $F_C$  corresponds to a delamination (opening and/or sliding) and not necessarily to a detachment (opening prevails on sliding). To distinguish between these two different mechanisms, we note that  $2\gamma = (K_{op}^2 + K_{sl}^2)/E \equiv 2(\gamma_{op} + \gamma_{sl})$ , where  $K_{op,sl}$  are the stress intensity factors at the tip of the interfacial crack for opening (mode I) or sliding (mode II) and  $K_{op} \propto F_{\perp} \propto \sin \vartheta$ , whereas  $K_{sl} \propto F_{\parallel} \propto \cos \vartheta$ ; assuming as a first approximation a detachment for  $K_{sl}/K_{op} \approx \tan^{-1} \vartheta < 1$  we derive a critical value of  $\sim 45^\circ$ . A similar behaviour has recently been confirmed by numerical simulations on gecko setae (Gao *et al* 2005): for

forces applied at an angle less than  $\sim 30^\circ$  the predominant failure mode was sliding, whereas larger angles correspond to detachment. Thus ‘friction’ (note here that the term friction does not invoke a ratio between a tangential and a normal force, but just the first one) is treated here as mode II of delamination, ie: sliding, and seems to have a fundamental role, as recently demonstrated on the basis of a force equilibrium rather than an energy balance (Tian *et al* 2006). However, imposing  $F_C(\vartheta = 0, \gamma_{op} = 0) = F_f \equiv \tau_f bc$  with  $\tau_f$  friction shear stress and  $c$  contact length, we find the correlation between sliding and friction in the form of  $\tau_f = 2c^{-1}\sqrt{\gamma_{sl}Eh}$ . Using the previous parameters we find  $F_C(\vartheta = 30^\circ)/F_C(\vartheta = 150^\circ) \approx 14$ , which can still be sufficient to control adhesion of non-ideal contacts, for which the strength is expected to be reduced by a factor of about one order of magnitude (Pugno 2006a). However, note that in any case (i.e. also at  $\vartheta \approx 0$ ) the total adhesive force could be overcome by subsequently detaching single points of contact and not the whole surface at once (Niederegger and Gorb 2003), even if, when not *in vivo*, this mechanism could be hard to activate. Note that the ratio predicted by equation (28) is compatible with home-made experiments that we have performed using adhesive tape. For larger thickness, the behaviour would be that of a beam rather than of a film (see the appendix).

## 7. Towards a Spiderman suit

According to our analysis, a man (palm surfaces of  $\sim 200 \text{ cm}^2$ ) and gecko-material gloves ( $\sigma_{\text{gecko}} \approx 0.58 \text{ MPa}$ ) could support a mass of  $\sim 1160 \text{ kg}$  (safety factor  $\sim 14$ ), or with spider-material gloves ( $\sigma_{\text{spider}} \approx 0.24 \text{ MPa}$ ) a mass of  $\sim 480 \text{ kg}$  (safety factor  $\sim 6$ ). Thus spiderman suits could become feasible in the near future. Note that theoretical van der Waals gloves ( $\sigma_{\text{vdW}}^{(\text{th})} \approx 20 \text{ MPa}$ ) would allow one to support a mass of  $\sim 40\,000 \text{ kg}$  (safety factor of  $\sim 500$ ). Carbon nanotubes could be one of the most promising candidates for our applications: on a small scale a carbon nanotube surface was able to achieve adhesive forces  $\sim 200$  times greater than those of gecko foot hairs (Yurdumakan *et al* 2005), even if it could not replicate large scale gecko adhesion, perhaps due to a lack of compliance and hierarchy. Thus, we propose the use of hierarchical branched long (to have sufficient compliance) nanotubes (Meng *et al* 2005) as good material for a Spiderman suit, with a number of hierarchical levels sufficient to activate self-cleaning, as quantifiable by our calculations. Their aspect ratio must not be too large, to avoid bunching (Hui *et al* 2002, Glassmaker *et al* 2004) and elastic self-collapse under their own weight, but sufficiently large to conform to a rough surface by buckling under the applied stress (see Bhushan and Sayer 2007), similar to the optimization done by nature in spiders and geckos. In particular, following Glassmaker *et al* (2004) and Yao and Gao (2006) for the bunching and introducing our result for the pillar radius at the level  $N$  ( $r_N = r_0(\varphi/n)^{N/2}$ ) we find the anti-bunching and anti-self-collapse (Timoshenko and Gere 1961) conditions at the hierarchical level  $N$  in the following form:

$$s < \min \left\{ 2 \left( \frac{3^3 \pi^4}{2^5 (1-v^2)} \right)^{1/12} \left( \frac{Er_0}{\gamma} \right)^{1/3} \left( \frac{\varphi}{n} \right)^{N/6} \left( \sqrt{(\varphi_{\text{max}}/\varphi^N) - 1} \right)^{1/2}, \right. \\ \left. \left( \frac{8\pi^2 E}{r_0(\varphi/n)^{N/2} \rho g} \right)^{1/3} \right\}, \quad (29)$$

where  $v$  is the Poisson’s ratio,  $\rho$  is the material density and  $\varphi_{\text{max}} = \pi/2\sqrt{3}$ ,  $\varphi_{\text{max}} = \pi/4$  or  $\varphi_{\text{max}} = \pi/3\sqrt{3}$  for triangular, square or hexagonal pillar lattices respectively. In order to have a uniform contact, the buckling (Timoshenko and Gere 1961) must be activated under the applied

stress  $\sigma_a$  (e.g.  $\sim 10$  kPa, see Bhushan and Sayer (2007)), thus imposing

$$s > \pi \sqrt{4/3} \varphi^{N/2} \sqrt{(\sigma_a/E)}; \quad (30)$$

equations (29) and (30) can be used for an optimal design of hierarchical superadhesive tissues.

Accompanied by large transparent (if not fully invisible, at the cost of a lower strength) nanotube-based cobwebs, a complete preliminary Spiderman suit could be realized.

## 8. Conclusions

We have proposed new laws to design futuristic self-cleaning, superadhesive and releasable hierarchical smart tissues, as well as large invisible cables, based on carbon nanotube technology. The analysis thus represents a first step towards the feasibility of a Spiderman suit.

## Acknowledgments

The author thanks Dorothy Hesson for the final English grammar supervision and MIUR and PROMOMAT for financial support.

## Appendix

Consider the delamination from a substrate of a linear elastic beam, subjected to a force  $F$  at its free end, inclined by an angle  $\vartheta$ ; the Young's modulus is denoted by  $E$ , the (free-) length is  $l$ , width  $b$ , height  $h$ , cross-sectional area  $A \equiv bh$  and moment of inertia  $I \equiv bh^3/12$ .

In linearity, the variation of the total potential energy  $\Phi$  during detachment will be, according to Clapeyron's theorem, equal to the opposite of the variation of the elastic strain energy  $\Psi$ ; for our system  $\Psi = F/(2E) \int_0^l (\sin^2 \vartheta/I + \cos^2 \vartheta/A) dz$ . Thus, the critical energy release rate can be evaluated by derivation with respect to the detached surface area, as  $2\gamma \equiv -d\Phi/(bdl) = d\Psi/(bdl)$ . For a discrete crack propagation the previous equation must be modified as  $2\gamma \equiv -\Delta\Phi/(b\Delta l) = \Delta\Psi/(b\Delta l)$  (Pugno and Ruoff 2004). Accordingly,

$$2\gamma = (\omega \sin^2 \vartheta + s^2 \cos^2 \vartheta) \frac{F^2 l^2}{2bEI}; \quad \omega = 1 + \frac{\Delta l}{l} + \frac{1}{3} \left( \frac{\Delta l}{l} \right)^2 \quad (A.1)$$

where  $s = \sqrt{I/A}/l$  is the beam slenderness and  $\omega$  represents the correction imposed by the quantization  $\Delta l \neq 0$  of the crack advancement. For  $l/\Delta l \ll 1$ ,  $\omega \rightarrow \infty$  and the continuous and discrete predictions diverge, whereas for  $l/\Delta l \gg 1$ ,  $\omega \rightarrow 1$  and they converge, as they must (corresponding principle). In particular, for  $l = 0$  we now predict a finite detachment force, or strength (as proposed in our asymptotic matching laws, see Gao *et al* (2005)), whereas continuous crack propagation would imply unreasonable infinite values. Moreover,  $F_n = n^\beta F_1 (b \rightarrow b/\sqrt{n})$  with  $\beta(l/\Delta l \rightarrow \infty) = 1/2$  but  $\beta(l/\Delta l \rightarrow 0) = 0$ , showing that the self-similar ( $b \propto l$ ) contact cannot be split *ad infinitum* to increase the strength. Note that treating a characteristic gecko seta with the previous model to get the gecko strength we need to assume  $\Delta l$  close to the spatula diameter, which coherently would represent in this context the contact quantum.

## References

- Arzt E, Gorb S and Spolenak R 2003 From micro to nano contacts in biological attachment devices *Proc. Natl Acad. Sci. USA* **100** 10603–6
- Autumn K, Liang Y A, Hsieh S T, Zesch W, Chan W P, Kenny T W, Fearing R and Full R J 2000 Adhesive force of a single gecko foot-hair *Nature* **405** 681–5

- Autumn K and Peattie A M 2002 Mechanisms of adhesion in geckos *Integr. Comp. Biol.* **42** 1081–90
- Autumn K, Sitti M, Liang Y A, Peattie A M, Hansen W R, Sponberg S, Kenny T W, Fearing R, Israelachvili J N and Full R J 2002 Evidence for van der Waals adhesion in gecko setae *Proc. Natl Acad. Sci. USA* **99** 12252–6
- Barthlott W and Neinhuis C 1997 Purity of scared lotus or escape from contamination in biological surfaces *Planta* **202** S1–8
- Bertram J E A and Gosline J M 1987 Functional design of horse hoof keratin: the modulation of mechanical properties through hydration effects *J. Exp. Biol.* **130** 121–36
- Bhushan B and Sayer A 2007 Gecko feet: natural attachment systems for smart adhesion *Applied Scanning Probe Methods* vol VII—*Biomimetics and Industrial Applications* (Berlin: Springer) pp 41–76
- Bushan B, Israelachvili J N and Landman U 1995 Nanotribology: friction, wear and lubrication at the atomic scale *Nature* **374** 607–16
- Bico J, Marzolin C and Quèrè D 1999 Pearl drops *Europhys. Lett.* **47** 220–6
- Bico J, Thiele U and Quèrè D 2002 Wetting of textured surfaces *Colloids Surf. A* **206** 41–6
- Blossey R 2003 Self-cleaning surfaces—virtual realities *Nat. Mater.* **2** 301–6
- Carpinteri A 1997 *Structural Mechanics: A Unified Approach* (London: Taylor & Francis)
- Carpinteri A and Pugno N 2005 Are the scaling laws on strength of solids related to mechanics of to geometry? *Nat. Mater.* **4** 421–3
- Cassie ABD and Baxter S 1944 Wettability of porous surfaces *Trans. Faraday Soc.* **40** 546–51
- Eisner T and Aneshansley D J 2000 Defense by foot adhesion in a beetle (*Hemisphaerota cyanea*) *Proc. Natl Acad. Sci. USA* **97** 6568–73
- Federle W, Rohrseitz K and Hölldobler B 2000 Attachment forces of ants measured with a centrifuge: better ‘wax-runners’ have a poorer attachment to a smooth surface *J. Exp. Biol.* **203** 505–12
- Gao H, Wang X, Yao H, Gorb S and Arzt E 2005 Mechanics of hierarchical adhesion structures of geckos *Mech. Mater.* **37** 275–85
- Gao X and Jiang L 2004 Biophysics: water-repellent legs of water striders *Nature* **432** 36
- Geim A K, Dubonos S V, Grigorieva I V, Novoselov K S, Zhukov A A and Shapoval S Y 2003 Microfabricated adhesive mimicking gecko foot-hair *Nat. Mater.* **2** 461–3
- Glassmaker N J, Jagota A, Hui C Y and Kim J 2004 Design of biomimetic fibrillar interface: 1. Making contact *J. R. Soc. Lond. Interface* **1** 23–33
- Hamaker H C 1937 The London-van der Waals attraction between spherical particles *Physica* **4** 1058–72
- Hansen W R and Autumn K 2005 Evidence for self-cleaning in gecko setae *Proc. Natl Acad. Sci. USA* **102** 385–9
- Huber G, Gorb S N, Spolenak R and Arzt E 2005a Resolving the nanoscale adhesion of individual gecko spatulae by atomic force microscopy *Biol. Lett.* **1** 2–4
- Huber G, Mantz H, Spolenak R, Mecke K, Jacobs K, Gorb S N and Arzt E 2005b Evidence for capillarity contributions to gecko adhesion from single spatula and nanomechanical measurements *Proc. Natl Acad. Sci. USA* **102** 16293–6
- Hui C Y, Jagota A, Lin Y Y and Kramer E J 2002 Constraints on micro-contact printing imposed by stamp deformation *Langmuir* **18** 1394–404
- Israelachvili J N 1991 *Intermolecular and Surface Forces with Application to Colloidal and Biological Systems (Colloid Science S)* (New York: Academic)
- Johnson K L, Kendall K and Roberts A D 1971 Surface energy and the contact of elastic solids *Proc. R. Soc. A* **324** 301–13
- Kendall K 1975 Thin-film peeling-elastic term *J. Phys. D: Appl. Phys.* **8** 1449–52
- Kesel A B, Martin A and Seidl T 2004 Getting a grip on spider attachment: an AFM approach to microstructure adhesion in arthropods *Smart Mater. Struct.* **13** 512–8
- Kretschmann D 2003 Velcro mechanics in wood *Nat. Mater.* **2** 775–6
- Laplace P S 1847 *Oeuvres Complètes* (Paris: Imprimerie Royale)
- Lau K K S, Bico J, Teo K B K, Chhowalla M, Amaratunga G A J, Milne W I, McKinley G H and Gleason K K 2003 Superhydrophobic carbon nanotube forests *Nano Lett.* **3** 1701–5
- Lee W, Jin M K, Yoo W C and Lee J K 2004 Nanostructuring of a polymeric substrate with well-defined nanometer-scale topography and tailored surface wettability *Langmuir* **20** 7665–9
- McFarlane J S and Tabor D 1950 Adhesion of solids and the effects of surface films *Proc. R. Soc. A* **202** 224–43
- Meng G, Jung Y J, Cao A, Vajtai R and Ajayan P M 2005 Controlled fabrication of hierarchically branched nanopores, nanotubes, and nanowires *Proc. Natl Acad. Sci. USA* **102** 7074–8
- Neinhuis C and Barthlott W 1997 Characterisation and distribution of water-repellent, self-cleaning plant surfaces *Ann. Bot.* **79** 667–77
- Niederregger S and Gorb S 2003 Tarsal movements in flies during leg attachment and detachment on a smooth substrate *J. Insect Physiol.* **49** 611–20

- Pugno N 2006a On the strength of the nanotube-based space elevator cable: from nanomechanics to megamechanics *J. Phys.: Condens. Matter* **18** S1971–90
- Pugno N 2006b Large invisible cables *Preprint cond-mat/0601369*
- Pugno N 2007 Velcro<sup>®</sup> nonlinear mechanics *Appl. Phys. Lett.* **90** 121918
- Pugno N and Ruoff R 2004 Quantized fracture mechanics *Phil. Mag.* **84** 2829–45
- Quéré D 2002 Fakir droplets *Nat. Mater.* **1** 14–5
- Quéré D 2005 Non-sticking drops *Rep. Prog. Phys.* **68** 2495–532
- Ruibla R and Ernst V 1965 The structure of the digital setae of lizards *J. Morph.* **117** 271–94
- Russell AP 1986 The morphological basis of weight-bearing in the scansors of the tokay gecko *Can. J. Zool.* **64** 948–55
- Schleich H H and Kästle W 1986 Ultrastrukturen an Gecko-Zehen *Amphib. Reptil.* **7** 141–66
- Stork N E 1983 Experimental analysis of adhesion of *Chrysolina polita* (Chrysomelidae: Coleoptera) on a variety of surfaces *J. Exp. Biol.* **88** 91–107
- Tian Y, Pesika N, Zeng H, Rosenberg K, Zhao B, McGuiggan P, Autumn K and Israelachvili J 2006 Adhesion and friction in gecko toe attachment and detachment *Proc. Natl Acad. Sci.* **103** 19320–5
- Timoshenko S P and Gere J M 1961 *Theory of Elastic Stability* (New York: McGraw-Hill)
- Wagner T, Neinhuis C and Barthlott W 1996 Wettability and contaminability of insect wings as a function of their surface sculpture *Acta Zool.* **77** 213–25
- Wenzel R N 1936 Resistance of solid surfaces to wetting by water *Ind. Eng. Chem.* **28** 988–94
- Wenzel R N 1949 Surface roughness and contact angle *J. Phys. Chem.* **53** 1466–70
- Yao H and Gao H 2006 Mechanics of robust and releasable adhesion in biology: bottom-up designed of hierarchical structures of gecko *J. Mech. Phys. Sol.* **54** 1120–46
- Young T 1805 An essay on the cohesion of fluids *Phil. Trans. R. Soc.* **95** 65–87
- Yu M F, Lourie O, Dyer M J, Moloni K, Kelly T F and Ruoff R S 2000 Strength and breaking mechanism of multiwalled carbon nanotubes under tensile load *Science* **287** 637–40
- Yurdumakan B, Raravikar N R, Ajayan P M and Dhinojwala A 2005 Synthetic gecko foot hairs from multiwalled carbon nanotubes *Chem. Commun.* **30** 3799–801
- Zhang M, Fang S, Zakhidov A A, Lee S B, Aliev A E, Williams C D, Atkinson K R and Baughman R H 2005 Strong, transparent, multifunctional, carbon nanotube sheets *Science* **309** 1215–9